On the morphology and structure of J-1 polymer, poly[(bis-4,4′-dicyclohexyl-methane) n-dodecanediamide], spherulites

L. S. Li and P. H. Geil*

Department of Materials Science and Engineering, University of Illinois at Urbana–Champaign, Urbana, IL 61801, USA

(Received 7 November 1989; revised 27 December 1989; accepted 19 January 1990)

Six different kinds of spherulites of du Pont's J-1 polymer, poly[(bis-4,4′-dicyclohexylmethane) n-dodecanediamide], were grown from an *m*-cresol solution during isothermal solvent evaporation. Polarizing microscopy shows different extinction patterns and interference colours in the spherulites. Electron diffraction indicates that three orthorhombic crystalline modifications with different ***a*** parameters exist in the single crystals and spherulites of J-1 polymer grown from solution. Electron microscopy and electron diffraction show that the variations in appearance of the spherulites are due to variations in the crystalline modifications and the crystallographic indices and morphology of the radiating crystalline entities.

(Keywords: spherulite structure; crystal structure; electron diffraction; poly[(bis-4-4′-dicyclohexylmethane)n-dodecanediamide])

INTRODUCTION

J-1 polymer (du Pont) has been proposed as a potential candidate for high-performance composites[1–5]. As shown by comparison of the X-ray[6] and electron diffraction patterns (below) of J-1 with a paper by Barton[7], J-1 is poly[(bis-4,4′-dicyclohexylmethane) n-dodecanediamide]:

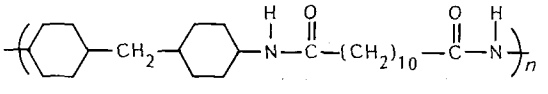

The rigidity of the chains induced by the cyclohexyl groups and intermolecular hydrogen bonding result in a high glass transition temperature ($T_g \simeq 145°C$) and melting point ($T_m \simeq 290°C$). On the other hand, the CH_2 segments introduce significant chain flexibility. As reported by Barton, for fibres[7], a result is polymorphism of crystal structure, a feature that we extend below. In addition the chain itself shows isomerization, the dicyclohexylmethane moiety being 55% *trans–trans* and 45% *cis–trans*[7]. Variation in morphological structure would also be expected and is found.

This work is part of a broad study of J-1 neat resin and J-1/graphite composites[6,8–12]. The original interest was to develop an understanding of the morphology of the resin in the composite and the effect on it of the graphite/J-1 interface. The results, however, are of significant interest in terms of understanding polymer crystal nucleation and spherulitic morphology in general. In particular, we show that six different types of J-1 spherulites can grow simultaneously during solvent evaporation, involving three different crystallographic unit cells, and that these unit cells all differ from that reported by Barton[7] and that found in quenched and then annealed samples[6].

Simultaneous growth of two types of spherulites has been reported for several polymers in the past, for instance for polypropylene crystallized from the melt[13]. In these cases the form of the spherulite has been proposed to depend on the nature of the (heterogeneous) nucleus, that form being propagated throughout the spherulite by a continuous crystallization process[14]. Random distribution of the nuclei results in random distribution of the spherulites. To the contrary, in J-1, the different types of spherulites are clustered, suggesting a different mechanism for determining the resultant spherulite morphology.

EXPERIMENTAL

Thin films of J-1 polymer were prepared by using a solution casting technique. A few drops of a hot solution (~200°C) of J-1 polymer (~0.2%) in *m*-cresol were deposited on the bottom of a small Petri dish, which had been pre-heated to one of several crystallization temperatures between 160° and 210°C. The dish was then maintained at the crystallization temperature until the solvent evaporated. The resulting thin film formed on the bottom of the Petri dish was slowly cooled to room temperature. Films deposited at the various temperatures were composed of single crystals and six different kinds of spherulites, the relative amounts of the different types of spherulites being dependent on the crystallization temperatures. The films were floated from the Petri dish using a 1% HF solution, rinsed several times in distilled water and were then picked up onto a microscope slide for the polarizing microscopy study. After careful examination and identification of the spherulites in the polarizing microscope, each film was cut into small pieces, refloated on distilled water, picked up on 3 mm copper grids and examined in a Philips 430 electron microscope at 200, 250 or 300 kV accelerating voltages.

* To whom correspondence should be addressed

0032-3861/91/0200384-07

The camera length for the electron diffraction analysis was calibrated using TlCl evaporated onto the films. Electron diffraction patterns were also obtained from the polymer sheared at 260°C between glass slides.

RESULTS AND DISCUSSION

In the following we discuss our observations for each of the six kinds of spherulites and associated single crystals individually, as well as for the sheared film.

Sheared films of J-1 polymer

Figure 1a is an electron diffraction pattern of a sheared film obtained at room temperature. *Figure 1b* is an electron diffraction pattern of the same film obtained at 263°C. This pattern (*Figure 1b*) shows that one of the strong sharp reflections on the equator of the pattern in *Figure 1a* has disappeared. This indicates that there are two crystalline modifications coexisting in the sheared sample. The reflections remaining at 263°C can be indexed by the orthorhombic unit-cell parameters described by Barton[7]; the reflection that disappears may correspond to one of his polymorphic forms. The observed *d*-spacings at room temperature and their indices are listed in *Table 1*.

Table 1

Equator					Meridian			
d (Å)	*h*	*k*	0		*d* (Å)	0	0	*l*
5.10	1	1	0	(orthorhombic)	11.15	0	0	4
4.66	2	0	0	(orthorhombic)	7.49	0	0	6
4.29	(second fibre form)				5.58	0	0	8
3.69	2	1	0	(orthorhombic)	4.46	0	0	10
2.18	3	2	0	(orthorhombic)	3.72	0	0	12
	4	1	0					

Spherulite with double concentric extinction rings

Figure 2a shows the appearance of these spherulites, obtained at 210°C, in the polarizing microscope under crossed polars. There is a Maltese cross extinction and double concentric extinction rings in each spherulite. After insertion of a compensator (Rot I) into the polarizing microscope, alternate blue and pink or orange interference colours along the radius of the spherulite from the centre to the periphery were observed. This indicates that the refractive indices vary periodically from $n_r > n_t$ (n_r is the refractive index in the direction parallel to the radius of the spherulite, while n_t is the refractive index in the direction perpendicular to the radius) through $n_r = n_t$ to $n_r < n_t$. When $n_r = n_t$ extinction takes place. This is the location at which an optic axis is parallel to the incident beam. According to the extinction pattern of the spherulite it is clear that there are two optic axes in the plane perpendicular to the radius of the spherulite.

Figure 2b is a transmission electron micrograph of a spherulite similar to that shown in *Figure 2a*. This figure shows that the spherulite is composed of radiating helical lamellae. *Figure 2c* is an electron diffraction pattern obtained from a sector of the spherulite. The arrow indicates the radius direction of the spherulite. The reflections in the pattern cannot be indexed by the unit-cell parameters obtained from X-ray fibre patterns[7]. Fortunately, there were some single-crystal-like regions in some of the thin films. *Figure 2d* is a single-crystal electron diffraction pattern from such an area. This

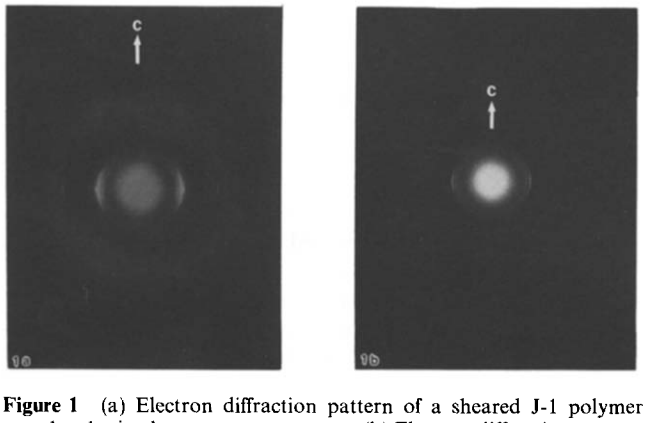

Figure 1 (a) Electron diffraction pattern of a sheared J-1 polymer sample, obtained at room temperature. (b) Electron diffraction pattern of the same sample as in (a), obtained at 263°C

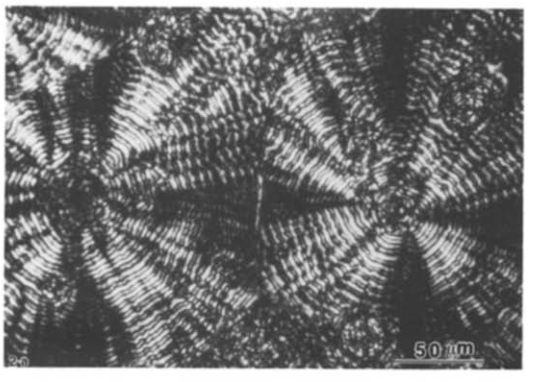

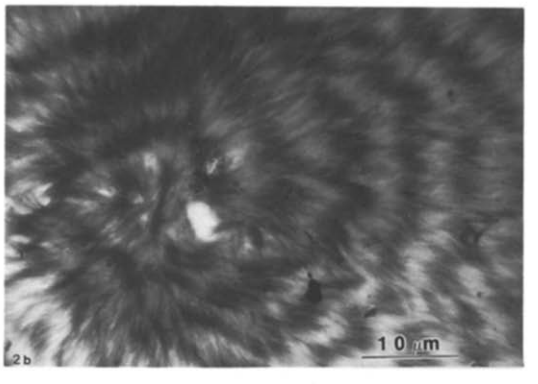

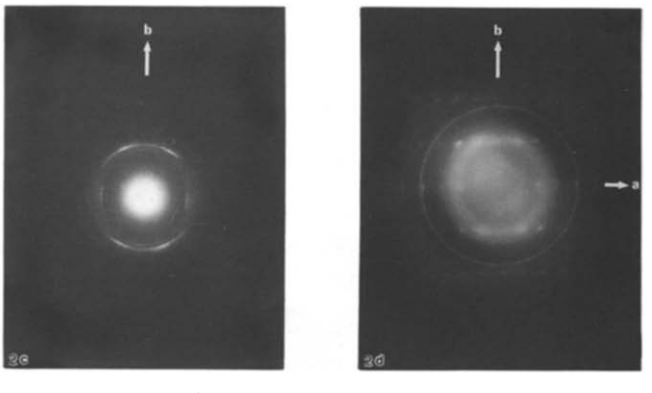

Figure 2 (a) Optical micrograph of spherulites with double concentric extinction rings (crossed polars). (b) Electron micrograph of a spherulite with double concentric extinction rings. (c) Selected-area electron diffraction pattern of the spherulite shown in (b). The arrow in this and subsequent patterns indicates the radius direction of the spherulite. (d) Electron diffraction pattern of a single crystal. (The ring is from TlCl)

Table 2

Equator (tangential)		Meridian (radius)		Off-meridian	
d (Å)	*h k l*	*d* (Å)	*h k l*	*d* (Å)	*h k l*
5.55	2 0 0_t, 2 0 1_t	4.96	0 1 0_t	4.53	1 1 0_t
5.21	2 0 3_t	2.48	0 2 0_t	4.32	1 1 3_t
4.94	2 0 4_t			3.65	2 1 2_t
4.45	2 0 6_t				

pattern shows an orthorhombic a^* b^* reciprocal lattice plane. The values of the a^* and b^* obtained from *Figure 2d* are different from those obtained from a fibre as reported by Barton[7] and from our sheared sample (*Figure 1a*). For this form c^* was determined by tilting the single crystal about the ***b*** axis; it agrees with the ***c*** axis spacing in the fibre patterns. The resulting unit-cell parameters of the single crystal are as follows. This type of crystalline structure of J-1 polymer is referred to as 'modification I'.

Modification I

$$a = 11.10\ \text{Å} \qquad b = 4.96\ \text{Å} \qquad c = 44.7\ \text{Å}$$

$$\alpha = \beta = \gamma = 90°$$

According to the parameters of modification I, the reflections of the electron diffraction pattern of the spherulite (*Figure 2c*) are easily indexed. The observed *d*-spacings and indices are listed in *Table 2*.

From *Table 2* it is clear that ***b*** is the radius direction of the spherulite. Therefore, the two optic axes are in the *ac* plane and the magnitude of the refractive index in ***b*** must be between the magnitudes of refractive indices in the ***c*** and ***a*** directions. It can be suggested that ***c*** is the direction with the largest refractive index, as in the case of e.g. poly(ethylene terephthalate)[15], and ***a*** is the direction with the smallest refractive index. According to the extinction pattern it is clear that ***c*** is the bisectrix of the acute angle between the two optic axes because the narrow spacing region between the extinction rings shows a blue interference colour in the first quadrant of the cross. The ***a*** is thus the bisectrix of the obtuse angle between the two optic axes. The acute angle is about 66°, which was estimated by the spacing between extinction rings. When the unit cell of J-1 polymer rotates around the ***b***, the refractive indices change from $n_r > n_t$ through $n_r = n_t$ to $n_r < n_t$. Therefore double extinction rings appear in the spherulite in the polarizing microscope under crossed polars.

Negative spherulite with single concentric extinction rings

Figure 3a is an optical micrograph of a second type of J-1 polymer spherulite, here obtained at 190°C. Each spherulite exhibits a Maltese cross extinction pattern and concentric extinction rings with equal spacing between them in the polarizing microscope under crossed polars. After insertion of the compensator (Rot I) the interference colour in the first and third diametrically opposed quadrants of the cross is orange and in the second and fourth ones is blue. This indicates that the spherulites are negative, but with concentric extinction rings. Therefore, the spherulite possesses a periodic radial structure with $n_r \leqslant n_t$. *Figure 3b* is a transmission electron micrograph of the spherulite, showing crystalline entities packed regularly around the centre of the spherulite. The morphology is quite different from that of the spherulite

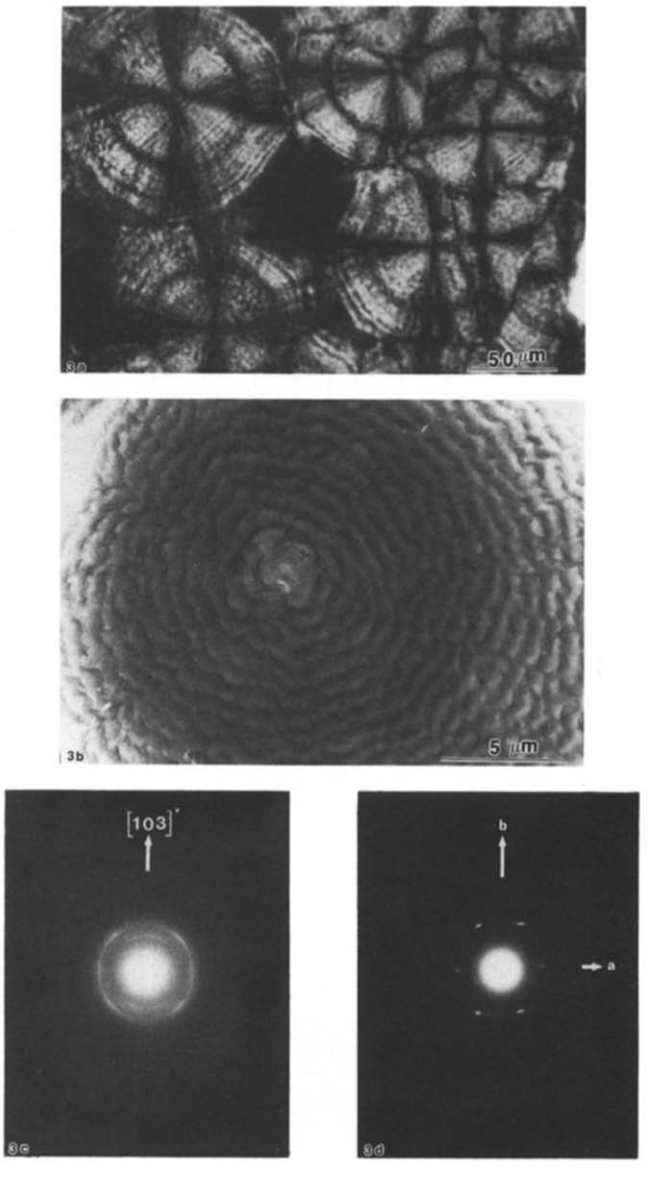

Figure 3 (a) Optical micrograph of negative spherulites with single concentric extinction rings (crossed polars). (b) Electron micrograph of a negative spherulite with single concentric extinction rings. (c) Selected-area electron diffraction pattern of the spherulite shown in (b). (d) Electron diffraction of a single crystal

with double concentric extinction rings shown in *Figure 2b*.

Figure 3c is an electron diffraction pattern obtained from a sector of the spherulite. The reflections of the pattern cannot be totally indexed by the unit-cell parameters of either the fibre patterns[7] or modification I. An electron diffraction pattern of a single-crystal-like region in the same film as the spherulites (*Figure 3d*) shows three reflections at the position of 2 0 0, one of which agrees with modification I, while at the position

of 0 1 0 only one reflection is shown. Based on this electron diffraction pattern two more crystalline modifications are determined:

Modification II

$a = 10.52$ Å $\quad b = 4.96$ Å $\quad c = 44.7$ Å

$\alpha = \beta = \gamma = 90°$

Modification III

$a = 9.64$ Å $\quad b = 4.96$ Å $\quad c = 44.7$ Å

$\alpha = \beta = \gamma = 90°$

The ***c*** parameters of these two modifications, which are around 44.7 Å, were not determined accurately due to the lack of sufficient sharpness of the $h\ 0\ l$ reflections during tilting the single crystal about ***b***. It is obvious that different modifications must be related to different conformations of the chains. Therefore, ***c*** parameters of these three modifications should be different. However, because the ***c*** parameters are very large, the deviations between the real values of ***c*** parameters and 44.7 Å are within the experimental error. Therefore, we tentatively adopt $c = 44.7$ Å for all of these three modifications. Because the ***b*** parameter is constant for these three modifications and the refractive index in the ***b*** is less than that in the ***c*** and larger than that in the ***a***, it can be suggested that ***b*** is the hydrogen-bond direction. It is noted the spacing in this direction is greater than the corresponding spacing (*a*-axis direction, 4.65 Å) in the fibre samples.

The reflections of the electron diffraction pattern of the spherulite (*Figure 3c*) can be indexed according to the parameters of modification III. The observed *d*-spacings and their indices are listed in *Table 3*.

The angle between the meridian (radius direction of the spherulite) and the reciprocal vector [1 0 6]* is $\sim 20°$. This indicates that [1 0 3]* is the radius direction of the spherulites. The angle between the [1 0 3]* and the ***a*** is 32.9° and the angle between the [1 0 3]* and the ***c*** is 57.1°; thus the angle between the two optic axes is 65.8°, which is consistent with the value measured from the narrow spacing of the concentric extinction rings of the first type of spherulite. When the unit cell of J-1 polymer rotates around [1 0 3]*, only one of the two optic axes can be parallel to the incident beam and the refractive indices vary periodically from $n_r < n_t$ to $n_r = n_t$ along the radius of the spherulite. This explains the presence of the single concentric extinction rings in the spherulite.

Positive spherulite

Figure 4a is an optical micrograph of a third type of

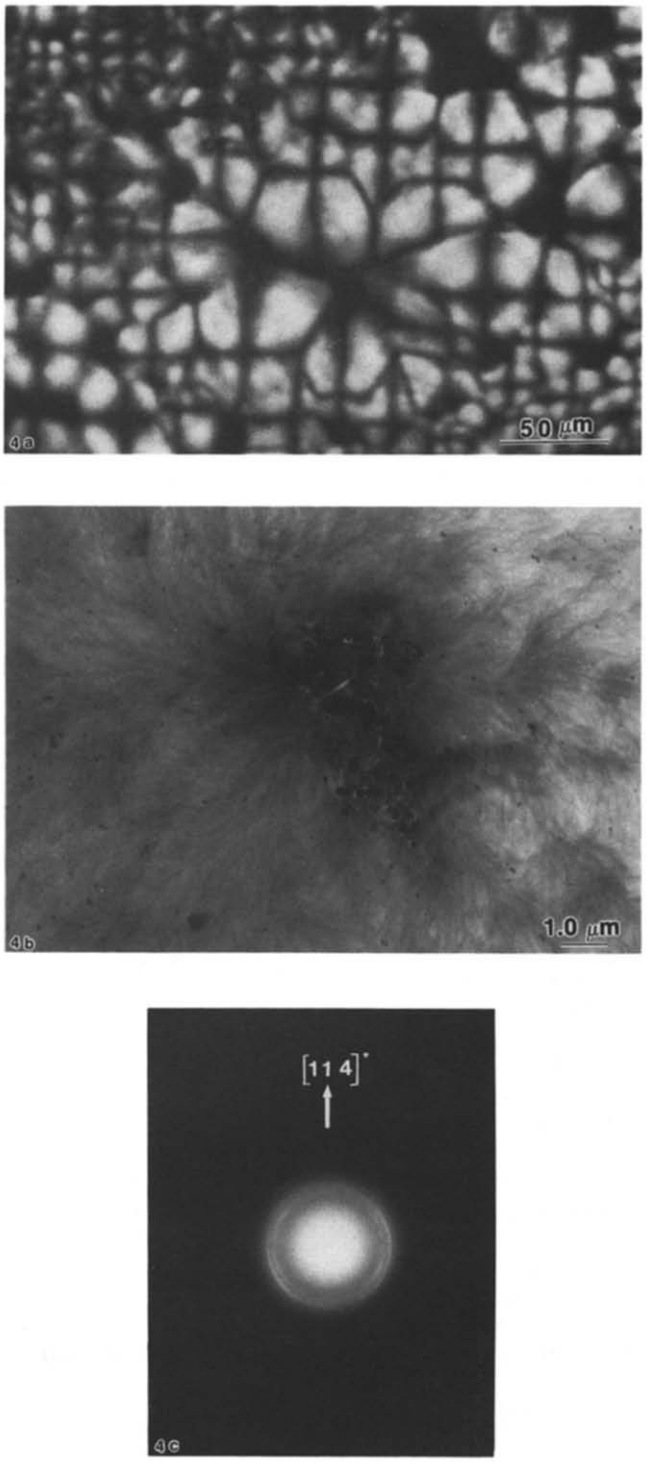

Figure 4 (a) Optical micrograph of positive spherulites (crossed polars). (b) Electron micrograph of a positive spherulite. (c) Selected-area electron diffraction pattern of the spherulite shown in (b)

Table 3

Meridian				Off-meridian				Off-equator			
d (Å)	*h*	*k*	*l*	*d* (Å)	*h*	*k*	*l*	*d* (Å)	*h*	*k*	*l*
4.73	0	1	3		1	1	0	5.89	1	0	6
				4.43	1	0	9				
					0	0	10				
				2.47	0	0	18				

J-1 polymer spherulite obtained at 180°C. This kind of spherulite shows a Maltese cross extinction in the polarizing microscope under crossed polars with no rings being visible. After insertion of the compensator the interference colour in the first and third quadrants of the cross is blue and in the second and fourth ones is orange, indicating a positive spherulite structure with $n_r > n_t$ everywhere. *Figure 4b* is a transmission electron micrograph of the spherulite. This figure shows that the spherulite is composed of feather-like crystallites.

Figure 4c is a selected-area electron diffraction pattern of the spherulite. Although it has considerably fewer reflections than the preceding patterns, the reflections in this pattern can be indexed by the orthorhombic unit cell of modification II. The observed off-equator *d*-spacings and indices are listed in *Table 4*. All other reflections are weak and difficult to measure.

The angle between the meridian and [2 0 1]* is 64°. This indicates that [1 1 4]* is probably the radius direction of the spherulite. The refractive index along the [1 1 4]* must always be larger than that in the tangential direction in the spherulite, yielding the positive spherulite.

Sunflower-like spherulite

Figure 5a shows sunflower-like spherulites obtained at 200°C. With insertion of the compensator into the polarizing microscope the interference colour changes alternately from blue to pink or vice versa in the central part of the spherulite. However, in the periphery the blue colour is exhibited in the first and third quadrants of the cross and orange colour is in the second and fourth ones. Electron microscopy indicates that the spherulite is actually composed of two kinds of spherulite structures: a spherulite structure with double concentric extinction rings in the central part of the spherulite and positive spherulite structure in the periphery of the spherulite (*Figure 5b*). The presence of such type of spherulite is probably because the parameters of ***b*** and ***c*** axes are almost the same in both crystalline structures (modification I and II); they can thus match each other on the (0 *k l*) planes.

Flower-like spherulite

Figure 6a shows flower-like spherulites coexisting with positive spherulites. The flower-like spherulites, obtained at 170°C, have much lower birefringence. Upon insertion of a compensator the blue and orange interference colours are irregularly distributed. An electron micrograph of the spherulite shows a radiating fibrillar morphology (*Figure 6b*). Electron diffraction patterns (*Figure 6c*) show increased diffuse scattering, indicating more disorder in the structure. There is only one reflection, with a spacing corresponding to 1 1 0 of modification I; however, because of the diffuseness, this designation, as to indices and modification, should be considered tentative. If correct, it appears that [1 1 0]* is the radius direction of the spherulite.

Table 4

Off-equator			
d (Å)	*h*	*k*	*l*
5.19	2	0	1
4.55	2	0	5

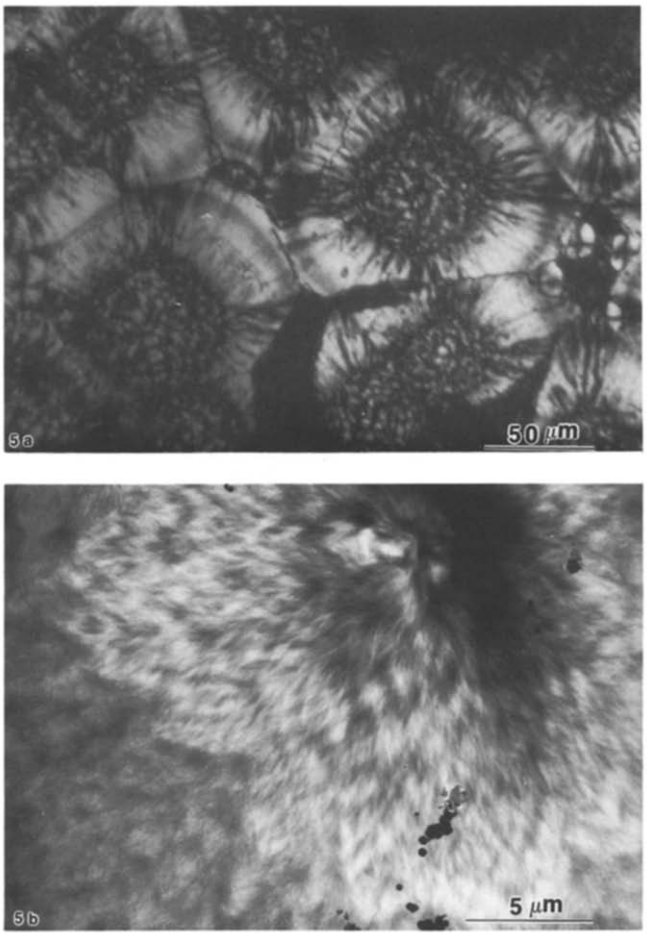

Figure 5 (a) Optical micrograph of sunflower-like spherulites (crossed polars). (b) Electron micrograph of a sunflower-like spherulite

Positive spherulite with coarse concentric extinction rings

Figure 7a shows spherulites with a Maltese cross extinction pattern and a series of coarse concentric extinction rings in each spherulite. They were obtained at 160°C. After insertion of a compensator into the polarizing microscope the interference colour in the first and third quadrants of the cross is blue and in the second and fourth ones is orange. This indicates a positive spherulite with $n_r \geq n_t$. *Figure 7b* is an electron micrograph of the spherulite. This figure shows concentric rings and tiny crystallites. The morphology is very different from all of those shown above.

Figure 7c is an electron diffraction pattern obtained from a sector of the spherulite. The reflections of the pattern can be indexed by the orthorhombic unit-cell parameters of modification II, the same as in the positive spherulites (type 3). The observed *d*-spacings and indices are listed in *Table 5*.

The angle between the meridian and the [0 1 4]* is ~25°. This indicates that the meridian is [1 1 3]*. Therefore, the radius direction of the spherulite is [1 1 3]*. When the unit cell of J-1 polymer rotates around [1 1 3]* one of the two optic axes must become parallel to the incident beam and the refractive indices vary periodically from $n_r > n_t$ to $n_r = n_t$. This explains the extinction pattern of the spherulite.

It is interesting to point out that the six different types of spherulites can grow simultaneously during solvent evaporation. Different types of spherulites usually are not

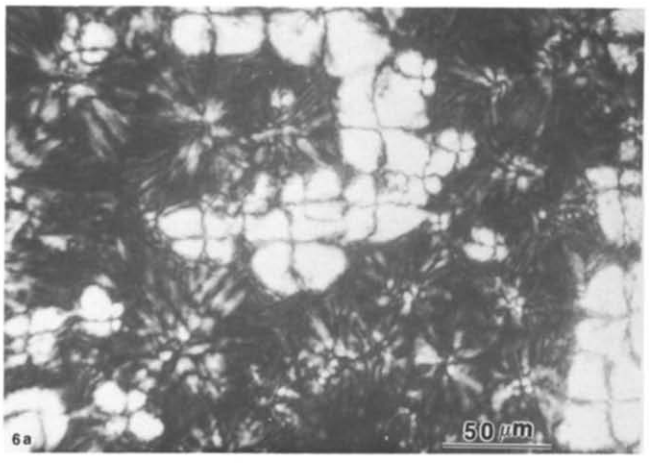

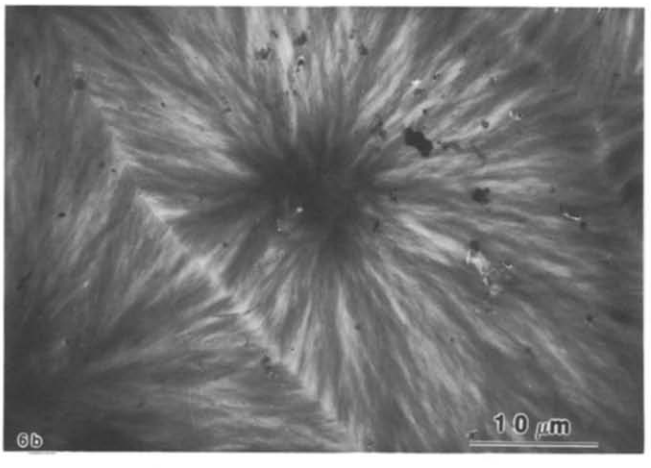

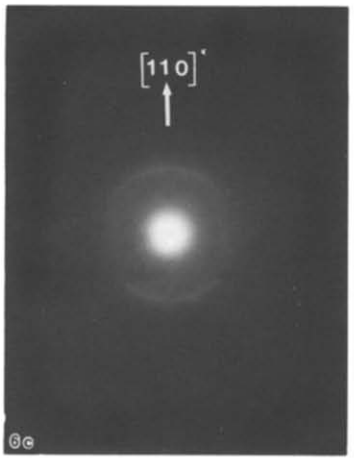

Figure 6 (a) Optical micrograph showing flower-like spherulites coexisting with positive spherulites (crossed polars). (b) Electron micrograph of the flower-like spherulites. (c) Selected-area electron diffraction pattern of a flower-like spherulite

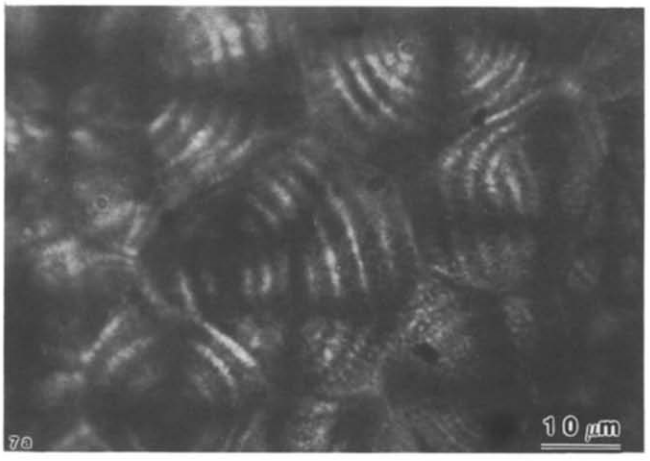

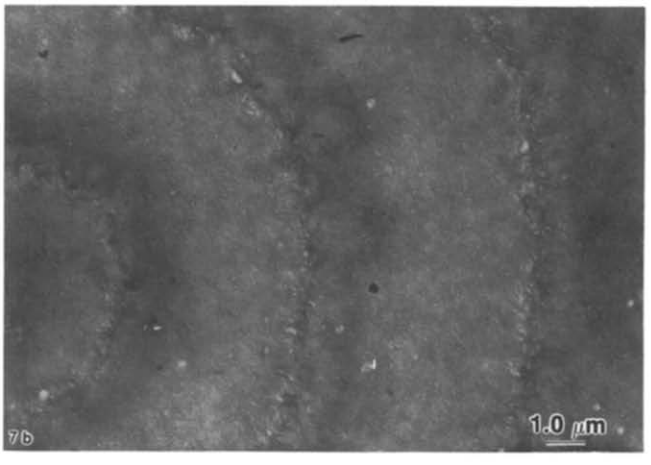

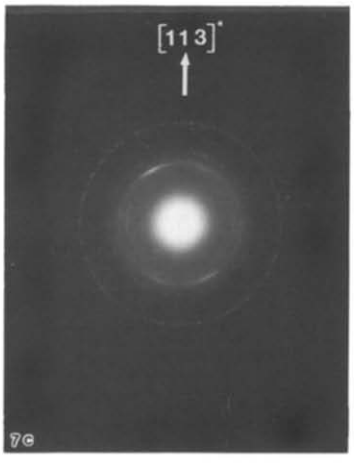

Figure 7 (a) Optical micrograph showing positive spherulites with coarse concentric extinction rings (crossed polars) coexisting with positive spherulites. (b) Electron micrograph showing a sector of a positive spherulite with coarse concentric extinction rings. (c) Selected-area electron diffraction pattern of the spherulite shown in (b). (The two rings are from TlCl)

Table 5

Off-meridian				Equator			
d (Å)	*h*	*k*	*l*	*d* (Å)	*h*	*k*	*l*
4.51	0	1	4	5.15	2	0	2

distributed at random; they are always clustered. The relative amounts of different types of spherulites are dependent on the crystallization temperatures. The favourable temperature for the growth of each type of spherulite has been indicated above. The spherulites with double concentric extinction rings are the most frequent type of spherulites. They can grow at any temperature in the range of 160 to 210°C. This is probably because the radius direction of the spherulite is the direction of the hydrogen bonds ***b***, which aids the growth of the spherulite.

The simultaneous growth of different types of spherulites may be related to segregation by molecular crystallizability during solvent evaporation, with the spherulite form being determined by the local polymer chemical structure, and by local fluctuations in temperature during

solvent evaporations. Heterogeneous nucleation, due to foreign particles, is not expected to be of concern; the nuclei of given types would not be expected to be clustered.

CONCLUSIONS

Six different kinds of spherulites of J-1 polymer are grown simultaneously from *m*-cresol solution during isothermal solvent evaporation. The relative amounts of the different kinds of spherulites are dependent on the crystallization temperatures. Single-crystal-like regions can be observed by electron diffraction in some thin regions of these samples.

Three orthorhombic crystal modifications, with the same value of ***b*** but different ***a*** parameters, have been identified and characterized in these samples. The ***b*** axis is suggested to be the hydrogen-bond direction, leading to its constant value. None of these modifications are the same as several modifications previously reported for drawn fibres and quenched samples.

Variations in morphological structure, crystal growth direction and unit cell lead to the various types of spherulites. Significant differences in apparent crystallinity (by electron diffraction) are found for the six types; their clustering by type suggests segregation by molecular crystallizability during solvent casting.

ACKNOWLEDGEMENT

This research was supported, in part, by the National Science Foundation through the University of Illinois Materials Research Laboratory.

REFERENCES

1 Chang, I. Y. *Compos. Sci. Tech.* 1985, **24**, 61
2 Su, K. B. Proc 5th Int. Conf. Compos. Mater. (Eds. W. C. Harrigan Jr, J. Strife and A. K. Dhingra), TMS-AIME, Warrendale, PA, 1985, p. 995
3 Nairn, J. A. and Zoller, P. Proc. 5th Int. Conf. Compos. Mater. (Eds. W. C. Harrigan Jr, J. Strife and A. K. Dhingra), TMS-AIME, Warrendale, PA, 1985, p. 931
4 Chang, I. Y. Proc. Japan–US Conf. Compos. Mater.–III, Composite '86: Recent Advances in Japan and the United States (Eds. K. Kawata, S. Umekawa and A. Kobayashi), Tokyo, 1986, p. 615
5 Wedgewood, A. R., Su, K. B. and Nairn, J. 19th Int. SAMPE Tech. Conf., Nation's Future Materials Needs (Eds. T. Lynch, J. Perish, T. Wolf and N. Rupert), 1987, p. 454
6 Chen, A. W.-L., Miyase, A., Wang, S. S. and Geil, P. H. *J. Compos. Mater.* submitted
7 Barton, R., Jr. *Bull. Am. Phys. Soc.* 1987, **32**, 701
8 Miyase, A., Chen, A. W.-L., Geil, P. H. and Wang, S. S. *J. Compos. Mater.* submitted
9 Miyase, A., Wang, S. S., Chen, A. W.-L. and Geil, P. H. *J. Compos. Mater.* submitted
10 Miyase, A. and Wang, S. S. *J. Compos. Mater.* submitted
11 Wang, S. S. and Desoutter, P. *Int. J. Fract.* in press
12 Wang, S. S. and Desoutter, P. *J. Compos. Mater.* in press
13 Keith, H. D., Padden, F. J., Jr and Keith, H. D. *J. Appl. Phys.* 1959, **30**, 1479; Keith, H. D., Padden, F. J., Jr, Walter, N. M. and Wyckoff, H. W. *J. Appl. Phys.* 1959, **30**, 1485
14 Geil, P. H. 'Polymer Single Crystals', Wiley-Interscience, New York, 1963, Ch. IV
15 Kunugi, T., Shiratori, K., Uematsu, K. and Hashimoto, M. *Polymer* 1979, **20**, 171